Wide-Angle X-ray Scattering of Random Metallocene−Ethylene Copolymers with Different Types and Concentration of Comonomer

A. G. Simanke and R. G. Alamo*

Florida Agricultural and Mechanical University and Florida State University, College of Engineering, Department of Chemical Engineering, 2525 Pottsdamer St., Tallahassee, Florida 32310-6046

G. B. Galland and R. S. Mauler

Instituto de Quimica, Universidade Federal do Rio Grande do Sul, Porto Alegre, Brazil

Received April 12, 2001

ABSTRACT: The WAXS diffractograms of random ethylene copolymers were analyzed for samples rapidly quenched, annealed, or isothermally crystallized. Comonomers studied include 1-decene, 1-hexene, 4-methylpentene, norbornene, and dicyclopentadiene in a range of concentration that includes semicrystalline and amorphous copolymers at ambient temperature. Only crystalline reflections corresponding to the orthorhombic structure were identified in these copolymers. Focus is given to analyze the contribution of the concentration of comonomer as well as the comonomer type in the angular position of the amorphous halo. For samples quenched to 23 °C the peak value scales linearly and in inverse proportion with the concentration of comonomer in the copolymer reflecting the increase of the average backbone carbon−carbon intermolecular distance associated with the interlamellar region. With increasing temperature, a progressive melting of crystallites changes the comonomer composition of the amorphous region and leads to a temperature coefficient of the peak position of the halo that is a function of the concentration of comonomer in the chain.

Introduction

Extracting the amorphous halo of wide-angle X-ray diffractograms of semicrystalline polymers has been a common subject of study in relation to the determination of the degree of crystallinity.[1−7] The X-ray halos of amorphous polyolefins contain, in the most intense low q range, two distinct maxima as documented by Turner-Jones.[8] The peak at low diffraction angle ($2\theta < 15°$), also called "prepeak" in recent studies,[9] was related to the average distance between carbon atoms of different main chains. There is a good correlation between side-chain length and the angular position of this peak. The peak at $2\theta = 19° \pm 2°$ represents both the intramolecular C−C bond distance and the short-range intermolecular van der Waals interactions. The WAXS profile of liquid linear polyethylene, devoid of branches, shows, in the same low q range, one amorphous halo where both intra- and intermolecular C−C distances are contributing. Other less intense peaks corresponding to different types of intramolecular distances are also present at $2\theta > 20°$.[9] The intermolecular contribution to the more intense amorphous peak of linear polyethylene ($2\theta \approx 18°$) is thought to be the main contribution to the halo. This correlation is based on the observed strong dependence of this peak with temperature while small variations were observed in the intramolecular component ($2\theta \approx 42°$).[8,10] It is of interest to investigate the effect of branching, concentration, and type on the average intermolecular distance in the amorphous region of linear low-density polyethylenes. This effect should be reflected in the angular position of the main halo. The halo and other diffraction peaks of the total diffractogram are usually extracted using some type of peak-fitting routines.[3,5,11−15]

* Corresponding author. E-mail address: alamo@eng.fsu.edu.

Investigations of the state of order or disorder of the intercrystalline region of linear polyethylenes and random ethylene copolymers have recently attracted interest.[15,16] The studies follow the general interest in fundamental and applied research on the new generation of metallocene-type polyolefins and also stem from the feasibility of the metallocene catalyst to control molecular weight and comonomer composition independently. Samples with a large variety of comonomer types and with a larger spectrum of molecular structure can now be studied.

Concerning the linear chains, neutron scattering studies of linear polyethylene[18] gave evidence by direct experimentation that the molecular conformation of the chains in the interlamellar region of solid samples had the same random coil dimensions as those in the melt. The experiments confirmed the prevailing view that, upon solidification of flexible chains, the random conformation was preserved in the amorphous region. However, the dissipation of order at the crystal−amorphous interface cannot be sharp, and a finite region of intermediate order has been documented in semicrystalline polymers.[19] In analyzing the WAXS profiles, the question that still prevails is how to account for this phase of intermediate order in the deconvolution of the amorphous and crystalline components of the total diffractogram. Different views have emerged among investigators despite using a similar type of deconvolution method, one that is based on a nonlinear least-squares minimization of the difference between the observed and calculated WAXS profiles. "Peak fitting" is carried out by electing the number of peaks to use in the profile and the peak functionality. For example, McFadding et al.[13] elected to include the loosely packed region as a second component of the amorphous halo and deconvoluted the total diffractogram using a four-band analysis. Their argument was based on experi-

10.1021/ma0106393 CCC: $20.00
Published on Web 08/21/2001

mental data that showed the peak value of the halo, below the melting point, of linear and branched polyethylenes, somewhere higher than the extrapolated values of the liquid polyethylenes at the same temperature. A similar conclusion was reached 20 years earlier by Ovchinnikov et al.,[20] who analyzed the intensities of oriented polyethylene using pole figure analysis. The latter authors concluded that there are two components contributing to the amorphous scattering: an isotropic component and a second one with a certain degree of texture.

Pole figure analyses were also carried out by Bartczak et al.[21] more recently to follow the molecular orientation of the amorphous region of linear polyethylene. The authors adapted a previously proposed model of two-dimensional molecular packing of chain segments in a pseudohexagonal arrangement[22−24] to interpret the development of texture in the amorphous region under deformation by plane-strain compression. A 6-fold symmetry of the pole figure obtained at the highest strain (1.86) supported the pseudohexagonal-type packing in the amorphous regions of the oriented sample. These data were further used to predict the molecular arrangement during deformation from the initial undeformed state, taking into account the connectivity of the molecules between amorphous and crystalline regions.[21] It was speculated that the two-dimensional arrays of parallel clusters of macromolecules (bundles) arranged in a hexagonal form may be present in the initially undeformed amorphous regions. However, the experimental data did not distinguish whether these clusters are specific to the region of intermediate order (interphase) or their location spans all the interlamellar region. The spatial random orientation of the crystallites and also a random orientation of the possible pseudohexagonal clusters of the undeformed sample lead to homogeneous pole figures for the crystal as well as for the amorphous region. Thus, there is the possibility that the final texture of the amorphous region developes from the formation of dimensionally small arrays that resemble the initial (undeformed) structure of the interface. The principal chain slip (100)[001] of the crystal during deformation, passed yield, will be readily transmitted along the (100) planes of the hexagonal domains and throughout the rest of the amorphous structure leading to a coherently aligned structure. Pseudohexagonal clusters need not be present in the amorphous regions of the undeformed polyethylene.

The interlamellar cluster model and the interpretation of the evolution of texture in the amorphous region of polyethylene by Bartczak et al.[21] are relevant in connection with recent works[16,25] in which a hexagonal structure is claimed to be present, in addition to the most common orthorhombic phase of polyethylenes, not only in oriented drawn fibers of ethylene−propylene copolymers[26] but also in deformed and undeformed ethylene−octene copolymers.[16] Thus, there is the question to what degree specific deconvolution methods can be used to characterize multiple phases and extract and quantify the diffraction pattern of the interfacial region.

An elaborate fitting procedure with up to seven pure Gaussian peaks has been used in a recent work[14] to fit the diffractogram of ethylene−octene copolymers at room temperature. These authors choose to fit the region of intermediate order as a second pair of ordered (110) and (200) reflections (at significantly different angular positions from the pure orthorhombic ones) for low branched copolymers and to the 19° 2θ region for copolymers with the highest concentration of branches (4.8 mol %). However, the basis for this distinction was not specified in this work.[14] Baker et al.[15] did not observe the pseudohexagonal phase and did not find enough justification to use four or more peaks in the fitting analysis, because the improvement in the fit compared to a three peaks analysis was negligible. However, they found a discrepancy in the crystalline peak positions between the low and high angle regions of the diffractograms. This discrepancy was found in oriented (fibers) and unoriented ethylene copolymers and was attributed to the presence of the partially ordered interfacial region. The diffractogram corresponding to this region of intermediate order was obtained by subtracting from the sample diffractogram those of the pure crystalline and amorphous regions. The resulting WAXS profile of the interface span over the whole 2θ region and was found to be closer to the crystalline spectrum than to the amorphous. This finding is in agreement with the results from a previous factor analysis study of the Raman spectra of linear polyethylenes.[27]

Additional reports analyzed the degree of conformational disorder in the interlamellar region by following changes in the disordered longitudinal acoustic mode (D-LAM) of linear polyethylene and model random ethylene copolymers.[28,29] It was quite evident that for the *linear chains* this band in solid samples had the same similarities as for the pure melt. The result indicated that the amorphous region of the bulk crystallized linear chain had the same random conformation as that of the molten sample in analogy to the neutron scattering results.[18] However, the frequency of the Raman D-LAM band of solid random ethylene copolymers increases with increasing branching content, indicating a clear effect of the branches on the chain conformation of the amorphous regions of these copolymers. The effect reflected a decrease in number of trans bonds and was in agreement with the measured and calculated decrease of the characteristic ratio of model copolymers with increasing comonomer content.[30,31] Compared to the linear chain, the conformation of the molecule of a random ethylene copolymer in the melt is less extended, becoming more compact with increasing branching content.

One could predict that the documented change of characteristic ratio with branching content in ethylene copolymers should cause differences in the intermolecular distance and, therefore, lead to some variation of the angular position and shape of the amorphous halo in the WAXS diffractograms. The main objective of this work is to investigate this correlation. To minimize complications in the interpretation of the data that could derive from a broad distribution of chain lengths or from a heterogeneous intermolecular comonomer composition, a series of homogeneous copolymers prepared with the same metallocene-type catalyst were used. In this work we also describe some of the subjectivity in relation to the peak-fitting and least-squares minimization procedure, especially on the basis of assigning the semiordered interfacial region to any specific region of the total diffractogram.

Experimental Part

Materials and Characterization. The ethylene copolymers used and characterization data for concentration of

Table 1. Molecular Characterization of Linear PE and Random Ethylene Copolymers

sample	comonomer	mol % branches[a]	M_w	M_w/M_n
LPE (Marlex)		0	150 000	6.0
ED1.6	1-decene	0.8	111 500	2.6
ED5.4	1-decene	2.7	56 700	2.2
ED10.8	1-decene	5.4	49 500	1.9
ED16.6	1-decene	8.3	67 400	2.5
EDCP3.5	dicyclopentadiene	1.75	142 500	3.5
EH9.5	1-hexene	4.75	109 000	2.0
E4MP14.0	4-methyl-1-pentene	7.0	29 600	2.0
ENB19.3	norbornene	9.65	106 100	2.9
d-HPBD[b]	ethyl branches	10.6	78 000	1.1

[a] Mol % branches per 100 backbone carbons. [b] Hydrogenated deuterated-polybutadiene.

comonomer and molecular weight are listed in Table 1. The ethylene copolymers were prepared using the metallocene catalytic system *rac*-Et[Ind]$_2$ZrCl$_2$/MAO as previously detailed.[32,33] Comonomers of the linear type (1-hexene, 1-decene), branched (4-methylpentene), and cyclic (norbornene and dicyclopentadiene) type were used. All polymerization reactions were carried out at 60 °C in a 1 L glass reactor equipped with a mechanical stirrer. Toluene, MAO, and the comonomer were added to the reactor under argon, the reaction medium was then saturated with ethylene, and the desired pressure was adjusted (1.6 bar). The copolymerization of ethylene and dicyclopentadiene was carried out at 30 °C. The reactions were initiated injecting the required amount of catalyst solution. After a total reaction time of 30 min, the polymer solution was poured into a HCl/methanol solution (1.5% v/v). The polymer was recovered by filtration, washed with ethanol and water, and dried in a vacuum until constant weight.

The molar mass of the copolymers was determined by gel permeation chromatography in a Waters 150 CV-plus System, equipped with an optic differential refractometer, model 150 C, and a set of three columns, Styragel HT type (HT3, HT4, HT6) calibrated with narrow molar mass distribution standards of polystyrene and polyethylene. 1,2,4-Trichlorobenzene was used as solvent. The measurements were carried out at 140 °C using a solvent volumetric flow rate of 1.0 mL/min.

The branching composition was determined by solution ^{13}C NMR in a Varian XL-300 spectrometer operating at 75 MHz. The measurements were performed at 80 or 120 °C with an acquisition time of 1.5 s, pulse width of 70°, and pulse delay of 5 s. The copolymers were dissolved in *o*-dichlorobenzene, and benzene-d_6 was used as an internal lock.

The linear polyethylene used is a commercial high-density polyethylene (LPE) made by the Phillips process (MARLEX). Also used was a deuterated polybutadiene with a high ethyl branching content (*d*-HPBD) and a labeling level of 40 ± 5%. This sample was obtained by anionic polymerization and was previously used in other works.[34] It is equivalent to a random ethylene−1-butene copolymer with very narrow molecular weight and intermolecular composition distributions. Both samples are also listed in Table 1.

Crystallization and Measurements. Most samples were studied under three different crystallizations. Films of 1 cm × 2 cm × 100 μm were prepared by compression molding the initial powder in a Carver press at 150 °C and rapidly quenching the molten polymer in water at 23 °C. These films will be referred as quenched samples and were analyzed within 2−4 h after quenching. The same films were annealed at 23 ± 1 °C for times that varied between 13 and 30 days; they will be referred as annealed samples. Three ethylene−decene copolymers were also isothermally crystallized at 63 °C (ED5.4), 70 °C (ED2.7), and 95 °C (ED0.8) in water or silicon oil thermostated baths. The crystallization temperatures were chosen from the DSC exothermic crystallization peak after cooling from the melt at 10 °C/min.

The X-ray diffraction patterns were recorded in reflection mode at room temperature using a Siemens D500 $\theta-2\theta$ diffractometer operating at 30 mA and 40 kV. Filtered Cu Kα radiation was used as the source. The diffraction scans were collected in a 2θ range between 5° and 45° and with 0.02° step size. The diffractometer was calibrated for *d* spacing with a standard polished piece of polycrystalline quartz, and the film thickness was offset using shims. Corrections for transparency were estimated negligible for the thin films used.[35] Diffraction patterns of the melt and partially molten samples were recorded at 150 and 90 °C, respectively, in reflection mode using a Siemens D500 $\theta-\theta$ diffractometer operating at 30 mA and 40 kV. The instrument has attached an Anton Paar HTK high-temperature head and uses filtered Cu Kα radiation as source. The equipment was calibrated with fine corundum powder (α-Al$_2$O$_3$), and the sample's height was appropriately adjusted. Temperature calibration was carried out using benzyl (mp 95 °C). The samples were heated (15 °C/min) from room temperature to 90 °C, and the temperature was stabilized for ∼10 min before the data were collected. The diffraction scans were acquired in a 2θ range from 5° to 45°, with a 0.02 ° step size. The sample was further heated to 150 °C, and the diffraction scans were acquired under the same conditions.

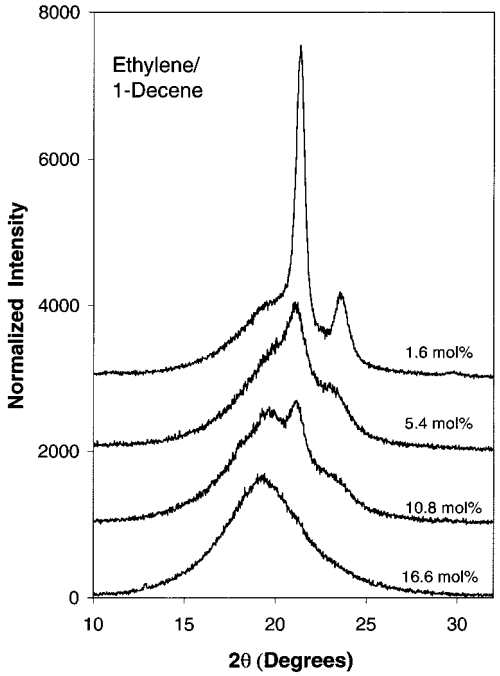

Figure 1. WAXS profiles of ethylene−1-decenes copolymers rapidly crystallized. The content of 1-decene is indicated. The profiles are normalized to the same total area.

The X-ray diffraction patterns were deconvoluted to separate the crystalline and noncrystalline components using the curve fit software package provided by the Graphic Relational Array Management System (GRAMS).[36] Mixed Gaussian and Lorentzian functions were used for the fit and the program adjusted the best combination of both types. The fitting procedure is based on area minimization through a nonlinear least-squares method.

The thermal behavior was analyzed by differential scanning calorimetry using a Perkin-Elmer DSC-7 under nitrogen and connected to an intracooler that allows subambient temperature control. The instrument was calibrated with indium. The samples were melted from −20 to 150 °C at a heating rate of 10 °C/min. The measured enthalpy of fusion was converted to the degree of crystallinity by taking 290 J/g as the enthalpy of fusion of a perfect polyethylene crystal.[37]

Results and Discussion

Quench Ethylene−1-Decene Copolymers. The effect of increasing comonomer content on the overall features of the WAXS diffractograms is shown in Figure 1 for the series of quenched ethylene−1-decene copolymers. The diffractograms were acquired at room tem-

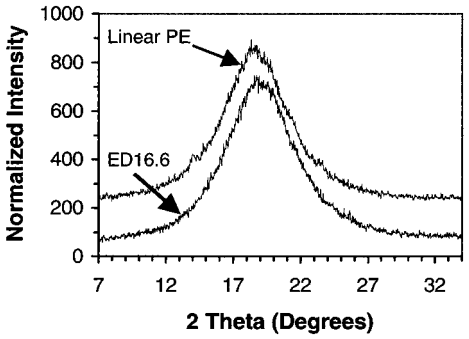

Figure 2. Area normalized WAXS profiles obtained at 150 °C for linear polyethylene (LPE) and ethylene−1-decene with 16.6 mol % 1-decene. The patterns have been displaced in the *y* axis.

perature and were normalized to the same total area using a linear background in a range of 2θ between 10° and 32°. The two strong reflections of the orthorhombic polyethylene cell, the (110) and (200) planes at 2θ values of 21.4° and 23.6°, are prominent in the WAXS pattern of the least branched copolymer. They decrease in intensity with increasing concentration of 1-decene in the copolymer paralleling a reduction in crystallinity caused by the increased number of noncrystallizable branches in the chain.[38]

The peak reflections of the (110) and (200) planes of ED5.4 and ED10.8 are shifted to lower values (2θ = 21.1° and 23.1°) compared to the peak of the lowest branched copolymer. This shift leads to the widely observed expansion of the *a*-axis and has been interpreted as a crystal strain effect caused by the accumulation of branches at the interphase of crystallites of very small thicknesses.[39−42] Other weak reflections characteristic of the orthorhombic (210), (020), and (310) planes are also observed at ~30° and (not shown) 36° and 40°.

The WAXS pattern of the copolymer with 16.6 mol % 1-decene did not show any crystalline reflection and a melting run by differential scanning calorimetry also lacked any observable endotherm at temperatures above 30 °C. On these bases the 16.6 mol % 1-decene copolymer is taken as amorphous at room temperature.

Initially one could think of using the diffractogram of the noncrystalline copolymer with 16.6 mol % decene as the amorphous halo to subtract from the total diffractogram of the semicrystalline copolymers in the analysis of the degree of crystallinity. However, as is implicit in Figure 1, not only the halo's peak maximum is shifted to lower values as branching content increases, but the shape of the halo may also be a function of the branching content in the amorphous region. Thus, both the width and 2θ peak of a broad halo of a semicrystalline copolymer are unknowns. A second consideration is that the actual comonomer content of the interlamellar region of these copolymers will be difficult to evaluate due to the nonequilibrium nature of the crystallization of these copolymers and the possibility of partial cocrystallization of both monomeric units.

A direct analysis of the effect of the comonomer composition on the halo of the diffractograms obtained at room temperature was not possible because a series of pure amorphous samples at room temperature with varied content of the same type of comonomer are not available. The effect can be analyzed at high temperature, and as an example, Figure 2 shows the diffractograms (at 150 °C) of the molten linear polyethylene and the 16.6 mol % ethylene−1-decene copolymer. The

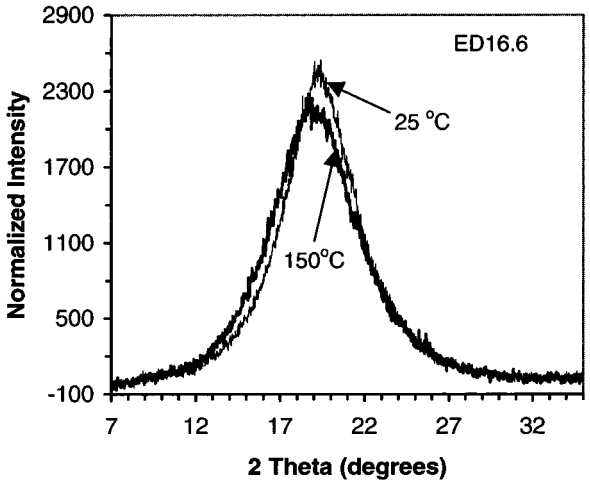

Figure 3. Comparison of area normalized WAXS profiles for ethylene−1-decene copolymer with 16.6 mol % 1-decene rapidly crystallized and measured at 25 °C and for the same sample measured at 150 °C. This copolymer lacks apparent crystallinity at 25 °C. Hence, the differences in profile shape and peak shift are caused by a decrease in density with temperature.

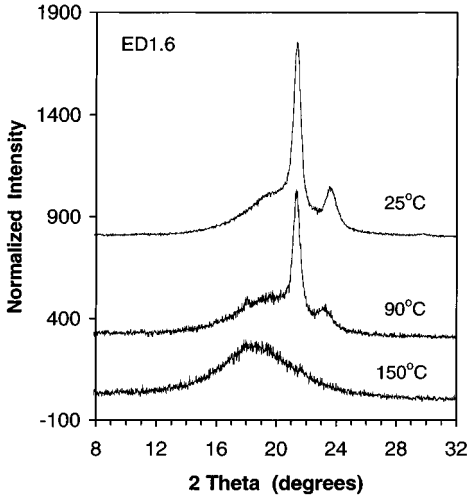

Figure 4. WAXS diffractograms of 1.6 mol % ethylene−1-decene rapidly crystallized and measured at the indicated temperatures.

comonomer addition leads to a shift in the peak and width of the halo.

Usual practice in extracting the amorphous halo from the diffractogram of the semicrystalline polymer is to use the shape of the scattering from the molten polymer properly scaled to the low angle region of the amorphous reflection. However, as seen in Figure 3 for the normalized diffractograms of amorphous ED16.6 at 25 and 150 °C, besides the reported peak shift, the density change with temperature also leads to changes in the width of the halo which are difficult to account for in the scaling. The effect of temperature on the angular position of the halo is also visually observed in Figure 4 for the diffractograms of the copolymer with the lowest decene content (1.6 mol %) recorded at 25, 90, and 150 °C. Inspection of the diffractograms at room temperature and at 90 °C also makes evident that the 2θ value of the crystalline reflections are basically independent of temperature, whereas the amorphous halo is very sensitive to temperature changes. The changes in the peak of the halo reflect a direct effect of the differing

van der Waals interactions as a consequence of both temperature and comonomer content variations. It is not possible to extract the peak value directly from the diffractogram because of the breath of the halo and overlap with more intense crystalline peaks. Thus, the quantitative determination of the peak of the halo of semicrystalline ethylene copolymers is complex. To find this value as a function of the comonomer content in the amorphous region, one could assume that all the branches are located in the intercrystalline region and use the level of crystallinity to calculate the concentration of comonomer in this region. The data of the liquid samples at high temperature can be used to obtain a 2θ halo/comonomer content calibration at 23 °C. The problem is that to determine the WAXS derived degree of crystallinity, the halo needs to be extracted for which knowledge of the peak position is required. Hence, the extraction of the amorphous component from the total WAXS diffractogram relied on peak-fitting and deconvolution procedures of the total diffractogram.

The type and shape function used in the fitting process were obtained from the following data. The crystalline 110 and 200 reflections of a high crystalline sample of linear polyethylene were fitted with curves that were approximately 50% mixed Gaussian and Lorentzian functions, in agreement with previous reported data.[35] On the other hand, the diffractograms of the amorphous copolymers obtained at either high or room temperature were invariably fitted to single curves that were >80% Lorentzian (with the fitting parameter $Chi^2 < 1$ and correlation > 0.99).[43] We should point out that the asymmetry reported by Monar et al.[14] in the diffractogram of molten polyethylenes was not observed in any of the samples studied here, and curve fitting to single or multiple pure Gaussian components (as suggested by these authors) led to rather poor fits in our copolymers.

On the basis of the results for the linear polyethylene with high crystallinity and those for the amorphous samples, the diffraction peaks were fitted in the range 5−35° of 2θ using mixed Gaussian and Lorentzian profiles. Mixed profiles were also the choice of other works.[13,15,25,35] Initially, an ideal two-phase structure of amorphous and crystalline components was assumed, and the diffractograms were fitted to a total of three peaks. The 2θ values of the (200) and (110) crystalline reflections were assigned to the peak values of the diffractogram and maintained fixed in the fitting process, whereas the peak of the amorphous region was let free. The program calculates the best fit to the area of the experimental diffractogram from an initial guess of the angular position of the peaks. In copolymers with low crystallinity for which the 2θ peak of the (200) reflection is not well-defined, such as ED10.8 of Figure 1, a profile was first obtained with a guess value for this peak. It was further observed that changing the fixed 2θ position around the calculated value did not have any significant effect on the final result of the profile. A representative example of a typical three-band profile analysis is given in Figure 5 for ethylene−1-decene with 5.4 mol % comonomer. Good fits were obtained for all the copolymers with correlation factors greater than 0.99 and a reduced chi^2 parameter that ranged between 0.5 and 0.98.

The values of the 2θ peak obtained from the three-peak fit analysis and the percent crystallinity, calculated as a ratio of the added areas of the (110) and (200) peaks to the sum of the areas of the three peaks, are given in Table 2. The crystallinity calculated from the heat of fusion is also listed. Data are given for samples rapidly quenched in water at 23 °C, annealed at 23 °C, and isothermally crystallized at the indicated temperatures. From the data of Table 2 we can first observe the shift of 2θ (110) and 2θ (200) to lower angular values with increasing comonomer content. The shift reflects the expansion of the orthorhombic unit cell amply reported in all types of random ethylene copolymers.[44−48] Except for small size branches that can be accommodated in the crystalline lattice such as methyl and chlorine[37] and have a direct large effect on the dimensions of the lattice, longer branches and those of the cyclic type which are not accommodated in the crystal lead to a similar small lattice expansion. For large volume branches the expansion is attributed to the strain that the branches conglomerated in the interphase cause to naturally thin crystallites.[38] The increase in the spacing of the (110) planes from $2\theta = 21.4°$ (4.14 Å) for quenched ED1.6 to $2\theta = 21.1°$ (4.20 Å) for quenched ED10.8 is very similar to that reported for 1-octadecene[48] and 1-octene[13] copolymers. The expansion observed in the (200) plane is also of the same magnitude as the reported one. The data of Table 2 also indicate that annealing the originally quenched crystallites or crystallization at lower undercoolings bring the 2θ crystalline diffractions to values closer to those of the homopolymer. Crystallite reorganization, thickening, or just the formation of thicker crystallites from the slower isothermal crystallization lead to a crystallite structure for which the effect on lattice expansion is considerably reduced compared to the less organized and thinner crystallites formed on quenching.

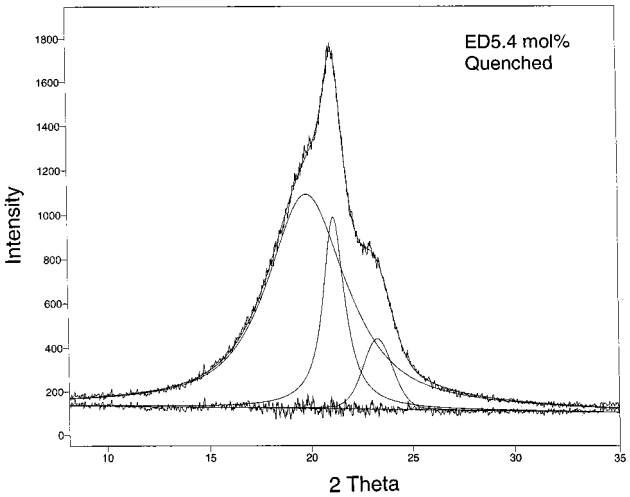

Figure 5. Nonlinear least-squares curve fitting to three peaks of the WAXS profile of quenched ethylene−1-decene with 5.4 mol % 1-decene. The difference between the experimental and calculated profiles is also given. Fitting parameters are $Chi^2 = 1.0$ and $R = 0.999$.

Independent of the method of determining the degree of crystallinity, from either the X-rays or heat of fusion, and for any crystallization mode, rapid quenching or isothermal crystallization, the crystalline fraction decreases rapidly with increasing comonomer content. This fact has been amply reported and reflects the role of noncrystallizable structural irregularities in reducing the average length of noninterrupted crystalline ethylene sequences. Using an *ideal* two-phase model, the X-ray-derived crystallinity changes from about 40% for the 1.6 mol % decene copolymer to ∼12% for the

Table 2. WAXS Data of Quenched, Annealed, and Isothermally Crystallized Ethylene−1-Decenes

mol % 1-decene	sample	$2\theta_{110}$	$2\theta_{200}$	X_c(WAXS)[a] (%)	2θ halo	$(1-\lambda)_{\Delta H}$[b] (%)
1.6	quenched in tap water	21.40	23.60	39.6	19.90	33.9
	annealed at 23 °C	21.44	23.72	46.0	19.90	42.4
	crystallized at 95 °C	21.41	23.69	50.0	19.80	39.1
5.4	quenched in tap water	21.10	23.13	23.4	19.80	22.4
	annealed at 23 °C	21.30	23.60	28.1	19.85	30.8
	crystallized at 70 °C	21.60	23.60	35.0	19.65	27.7
10.8	quenched in tap water	21.10	23.00	11.9	19.55	6.2
	annealed at 23 °C	21.10	23.10	11.8	19.50	12.3
	crystallized at 63 °C	21.30	23.30	12.9	19.40	11.2
16.6	quenched in tap water				19.35	0.7
	annealed at 23 °C				19.40	1.6

[a] Crystallinity calculated from WAXS diffractograms. [b] Crystallinity calculated from heat of fusion measurements.

copolymer with 10.8 mol % decene. As seen in Table 2, annealing at room temperature or isothermal crystallization increases significantly the X-ray crystallinity values of the least branched copolymers, but the effect is negligible for the highly branched copolymers. From previous kinetic studies of model random ethylene copolymers,[49] it is known that the actual crystallinity developed at the isothermal crystallization temperature is much lower than the value developed on quenching. The reason is the increase in the ethylene sequence length with decreasing undercooling that is required to form a stable crystallite and the concomitant reduction in the number of sequences of this length and longer ones in the copolymer chain.[49] After isothermal crystallization shorter sequences crystallize on cooling. The increased crystallinity of isothermally crystallized samples compared to the quenched values is attributed to a reduction in chain folding during formation of crystallites at the isothermal crystallization.

The DSC derived crystallinity values of most of the copolymers listed in Table 2 are lower than the X-ray crystallinities. Differences in crystallinity from measurements using different techniques have been reported before[50] and are attributed to the fact that any specific measurement may emphasize a given region of the phase structure. For example, the enthalpic change in disordering the partially ordered interfacial region may be negligible compared to the large change in enthalpy from melting crystallites. However, isolated ordered domains in the interface could contribute to the WAXS crystalline diffraction. Nevertheless, a direct comparison of the WAXS and DSC crystallinity data listed in Table 2 requires some discussion of how the DSC measurements were obtained. Since naturally the copolymers show broad melting transitions, and for the highly branched copolymers span temperatures as low as 10 °C, the melting scan was started at −20 °C and the heat of fusion evaluated in a temperature range from 5 °C to the last melting trace. Thus, the measured heat of fusion includes the fraction of crystallites formed from room temperature to 5 °C, whereas the X-ray room temperature measurement does not include this fraction. For comparative purposes the crystallinity $(1-\lambda)_{\Delta H}$ listed in Table 2 is a high value. On the other hand, corrections to the heat of fusion per gram of crystalline units (290 J/g) from the fact that copolymers melt in a broad temperature range far from the equilibrium value could lead, according to Mathot et al.,[51,52] to significantly higher crystallinity values. Hence, the $(1-\lambda)_{\Delta H}$ data of Table 2 may reflect cancellation of these effects.

Differences in the X-ray and DSC crystallinities could also arise from the contribution of the interphase. On this basis we also investigated the possibility of fitting the diffractogram with an extra component, and following the approach of McFaddin et al.,[13] we assumed that the contribution of the semiordered region (fourth peak in the fitting) is located in the region of the amorphous halo. The 2θ of the crystalline reflections were used as fixed values, and mixed Gaussian and Lorentzian profiles were used for all the peaks. A drawback from the increased number of degrees of freedom is the possibility of multiple minima in 2θ regions close to the region of iteration. Hence, depending on the starting guess values of the two components within the amorphous halo, significantly different fitting profiles were obtained, many of them with similarly good minimization parameters. Parts a and b of Figure 6 are examples of some of the profiles obtained for the same annealed ED5.4 copolymer. The drift in peak profiles to accommodate values of the parameters that correspond to a minimum well is obvious in these figures. The drift is avoided constraining the 2θ peak region of the "desired" two peaks within the halo, but we did not find good structural bases to apply this constrain. Baker et al.[15] also observed that the fitting routine with an extra peak did not lead to any improvement over the three-peak fit and, as for the copolymers of this study, led to correlation factors and reduced chi^2 as good as those obtained in the three-peak method. The need to constrain the variance was also acknowledged by Monar et al.[14] in their pure Gaussian multiple profiles fitting method, but it was not mentioned by Russell et al.[12,13] whose method seems very similar to the one we followed here. Moreover, from a previous factor analysis work,[27] and in line with the conclusion of Baker et al.,[15] it is reasonable to expect contributions of the interphase in the whole region of the diffractogram and not limited to a particular shape or angular region. This is due to the conformationally diffuse nature of the interface, for example, in terms of dissipation of trans−trans bonds from the ordered side of the interface to the disordered side.

On the basis of the need to arbitrarily set the region of the diffractogram and other features of the peaks corresponding to the amorphous and interfacial regions, we abandoned the four-peak fitting method. Focus was given to analyze systematic changes observed in the angular position of the amorphous halo obtained from the ideal two-phase model, i.e., the 2θ halo values listed in Table 2.

The variation of the 2θ halo with the average 1-decene content in the chain is plotted in Figure 7a for the quenched, annealed, and isothermally crystallized samples. The peak value of the amorphous halo scales linearly with the concentration of decene for the quenched samples and extrapolates, at comonomer concentration

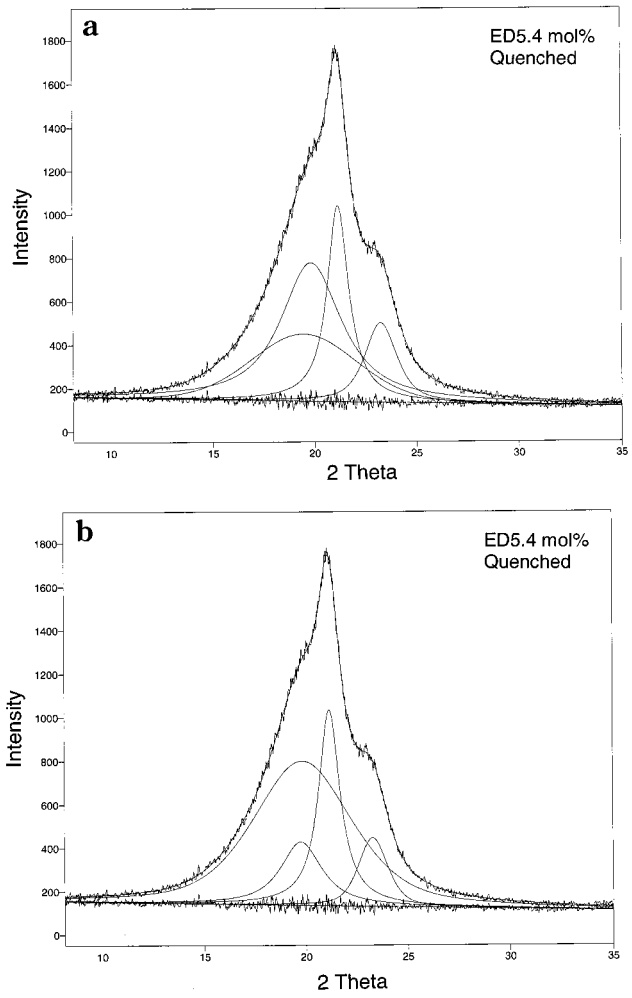

Figure 6. Nonlinear least-squares curve fitting to four peaks of the WAXS profile of quenched ethylene−1-decene with 5.4 mol % 1-decene. The difference between the experimental and calculated profiles is also given. (A) Fitting parameters are $Chi^2 = 0.95$ and $R = 0.999$. (B) Fitting parameters are $Chi^2 = 0.94$ and $R = 0.999$.

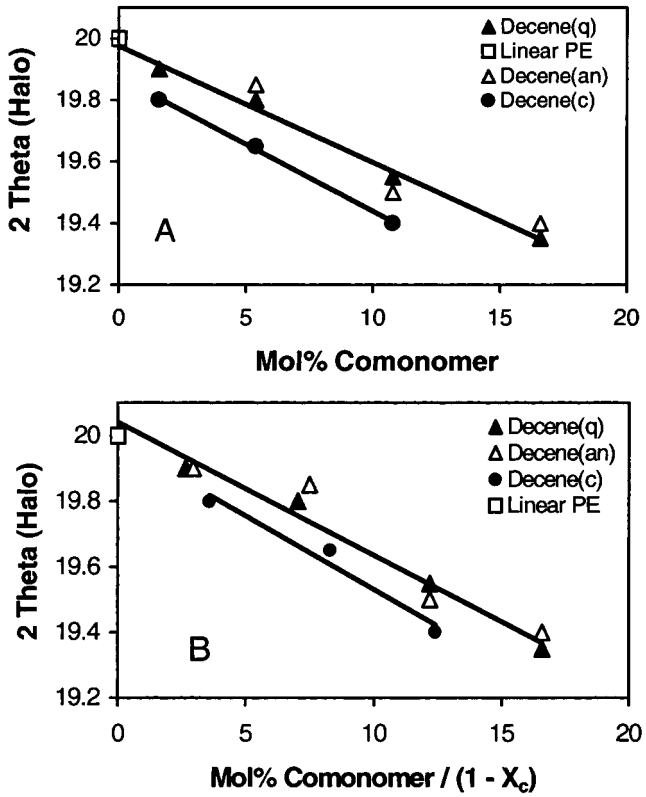

Figure 7. (A) Variation of 2θ halo peak (measured at room temperature) for ethylene−1-decene copolymers quenched (q), annealed (an), or isothermally crystallized (c). The value for the linear polymer is also plotted. (B) 2θ halo peak vs the concentration of comonomer in the intercrystalline region. Crystallinity is not detected for the 16.6 mol % copolymer at room temperature.

zero, to the value obtained for the linear polyethylene. The extrapolated value for 100% comonomer content is only about 1° below the value of 17.7° reported by Turner-Jones for amorphous isotactic poly-1-decene.[8] The agreement of the extrapolated values with those for the unbranched and 100% branched molecules is remarkable and reflects the contribution of the branch in the scattering of the amorphous region. Assuming that the octyl branch does not cocrystallize, the concentration of 1-decene in the intercrystalline region can be obtained correcting the average chain concentration with the X-ray crystallinity. In Figure 7b the 2θ halo is plotted vs the corrected concentration. As expected, there is less discrimination between quench and isothermally crystallized copolymers, and the extrapolated pure component values (20.05° and 16.1°) are also very close to the experimental data. In this comonomer concentration range, the quantitative change in intermolecular distance can be given by the linear dependence of the peak 2θ halo on the average molar concentration of 1-decenes (X_b), expressed according to Figure 7a as $2\theta_{(halo)} = -0.038X_b + 19.98$, for rapidly crystallized samples at 23 °C. For the intercrystalline region, the linear dependence of the 2θ halo for quenched samples (Figure 7b) has a slope of −0.040 and intercept of 20.04. Changes in the intercrystalline region with increasing comonomer content also led to an increase of the full width at half-height of the halo of about 0.5° with increasing comonomer in the ethylene−1-decene series.

Increasing the concentration of decene increases the average intermolecular distance between carbons of the main chain which in the amorphous random coil are separated by the octyl branch. The variation of 2θ halo in Figure 7 corresponds to the expected densification of the intercrystalline structure with increasing branch content, the overall dimensions corresponding to a more compact molecule compared to the linear unbranched chain. Thus, the experimentally measured densities of the melts of model random ethylene copolymers were found to increase with increasing branching content;[53] these data are contrary to some speculations[14] but in complete agreement with the expectations from the data of Figure 7. In addition to the density variation, measured and calculated characteristic ratios confirm the 2θ halo−intermolecular distance relationship. The characteristic ratios of two hydrogenated polybutadienes were found to decrease from 6.4 to 5.5 with increasing ethyl branches from 15 to ∼50 mol %.[30] They support calculations based on rotational isomeric state theory of the unperturbed dimensions of the same type of copolymers.[31] According to this calculation, the characteristic ratio (C^∞) decreases monotonically with increasing branching as a consequence of a decrease in the number of trans bonds in the main chain. In the whole compositional range, the experimental densities[53] and calculated C^∞ data[31] can be fitted by second-order polynomials as ρ (g/cm^3) $= -8 \times 10^{-6}X_b^2 + 8 \times 10^4X_b +$

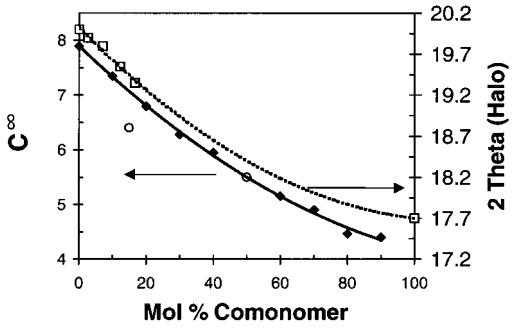

Figure 8. Change in calculated characteristic ratio for random ethylene−l-butene copolymers[53] (◆) and experimental C^∞ data from ref 31 (○) with increasing comonomer content. The variation of 2θ halo for ethylene−l-decene given in Figure 7b and the value for amorphous poly-l-decene can be fitted to a similar quadratic expression (□) (2θ halo $= 0.0002X_b^2 - 0.0417X_b + 20.02$).

0.7839 (ρ measured at 140 °C) and $C^\infty = 2 \times 10^{-4}X_b^2 - 5.8 \times 10^{-2}X_b + 7.9$ as is shown in Figure 8. The dotted line of this figure also indicates that a similar quadratic variation can be speculated to be followed for 2θ halo, in the whole comonomer content, when the data for amorphous isotactic poly(1-decene) is considered. However, further experimental data are needed to confirm a parallel quantitative relation between the change in C^∞ and the dependence on comonomer content of 2θ halo. The quadratic expressions of C^∞ and ρ can be approximated to linear relations for $X_b < 40$ mol %. In this range of comonomer content, the variation of C^∞ and 2θ halo is similar and corresponds to slopes of $\partial C^\infty/\partial X_b = -0.049$ and $\partial(2\theta \text{ halo})/\partial X_b = -0.040$, respectively, indicating that both dependencies have the same origin, a change in average molecular conformation. On a quantitative basis, a change in comonomer content between 1 and 16 mol % leads to an increase of intermolecular distance in the intercrystalline amorphous regions that corresponds to a 2θ halo change from 20° to 19.3° and to a change in characteristic ratio from 7.85 to 7.02. A reduction in trans bonds is also manifested in changes in the disordered longitudinal acoustic low-frequency mode of the Raman spectrum of similarly constituted copolymers,[29] whereas the frequency of the DLAM is unaffected by crystallinity changes in the unbranched polyethylene chain.[28]

The above series of experimental data and calculations corroborate the numerical data obtained from WAXS (Figure 7), indicating that the changes that shift the peak of the amorphous halo in ethylene copolymers are a direct consequence of the contribution of the branch to the scattering of this region. This relation opens the possibility to use the angular position of the amorphous halo to predict the effect of the comonomer in decreasing the probability of trans placements in the intercrystalline region of semicrystalline linear low-density polyethylenes.

In analyzing Figure 7a,b, we should also consider the possibility that, with increasing overall comonomer content in the chain, the concentration of defects in the crystal−amorphous interphase may increase. However, the effect of the semiordered diffuse interphase on the observed 2θ amorphous must be small because the data of Figure 7, although not extensive, are representative of crystalline and noncrystalline copolymers, and they do not show any discontinuity between the semicrystalline and the amorphous ethylene−decene copolymers. Traces of crystallinity were not observed at room temperature for ED16.6; thus, issues of interphase are not relevant for this copolymer.

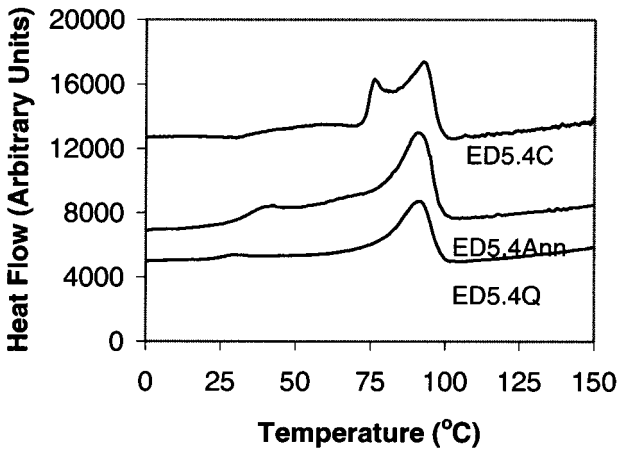

Figure 9. DSC melting thermograms of ethylene−1-decene (5.4 mol % 1-decene) quenched from the melt to 23 °C (lower endotherm), annealed at 23 °C for one month (middle), and isothermally crystallized at 70 °C (top).

Annealed and Isothermally Crystallized Copolymers. The three ethylene−1-decene copolymers with the lowest branch content were also isothermally crystallized at the temperatures indicated in Table 2. After crystallization had ellapsed, the samples were quenched in water at 23 °C and the diffractograms collected at room temperature. They were also fitted to three peaks to extract the angular position of the halo. For a comparison with quench and annealed samples, the data were also plotted in Figure 7. For all the ethylene−decenes analyzed the 2θ halo peaks are systematically between 0.1° and 0.15° lower than the values obtained for the quenched samples. This variation follows from the expected increase in branching composition in the interlamellar region, due to the increased crystallinity, from that acquired upon quenching (see Table 2). Hence, both quenched and isothermally crystallized samples show values of 2θ halo in a scale inversely proportional to the overall comonomer concentration. However, the trend in 2θ halo for isothermally crystallized samples is no longer linear in the compositional range studied. With respect to the overall chain concentration, isothermal crystallization leads to a larger change in comonomer content in the interlamellar region than for the quenched ones, whereas the amorphous copolymer is not subject to any compositional changes.

The results of the annealed samples are also of interest in relation to a recent DSC study[17] of similarly constituted ethylene−octene copolymers. The authors identified the development with time of a second lower temperature endotherm with the fusion of fringed micelle type crystallites formed in the intercrystalline regions of the primary formed crystals. Moreover, the increase in temperature of this endotherm with time was associated with a gradual decrease in the molar conformational entropy of the residual melt. We investigated whether the speculated melt entropy change was manifested in a change in the angular position and width of the halo in the copolymers studied here. As an example, Figure 9 shows the DSC melting thermograms of ED5.4 freshly quenched, after annealing at 23 ± 1 °C for 30 days and after crystallization at 70 °C followed by quenching. Room temperature annealing induced some changes in the structure, leading to an additional endothermic transition at about 35 °C. The melting peak

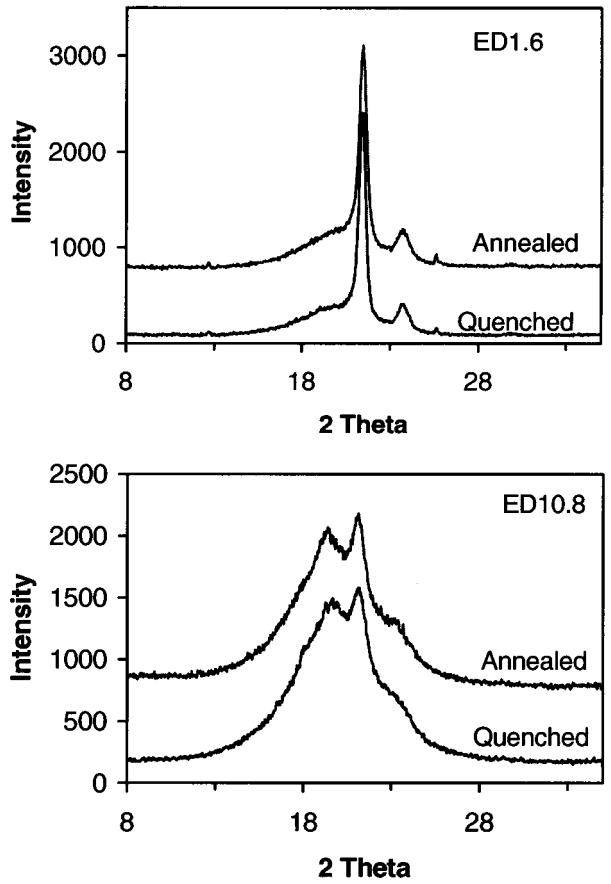

Figure 10. WAXS diffractograms for quenched and annealed ethylene−1-decene (1.6 mol % 1-decene) and ethylene−1-decene (10.8 mol % 1-decene). The diffractograms of the annealed samples are displaced in the *y* axis to facilitate distinction with those of the quenched samples.

and heat of fusion of this transition increase with annealing time[54] in analogy to the previous study.[17] However, the WAXS diffractograms of quenched and annealed copolymers showed insignificant differences. As seen in Table 2 and Figure 10, the 2θ halo data for annealed ethylene−1-decenes show small (<0.5°) and no systematic variations with respect to the value of the quenched samples. It is thus concluded that room temperature annealing does not lead to entropy changes in the melt that could significantly affect the WAXS diffractogram, especially in relation to the amorphous halo.

The WAXS diffractograms of quenched and annealed ethylene copolymers with different comonomer types were also analyzed. The comonomer type varied in a manner such that the linear (1-hexene), branched (4-methyl-1-pentene), and cyclic (norbornene and dicyclopentadiene) types were comparatively analyzed. The WAXS diffractograms of the quenched copolymers are shown in Figure 11, and the results of a three peaks fitting analysis are listed in Table 3. All the copolymers show some crystallinity measured by DSC except for quench deuterated HPBD (10.6 mol % ethyl branches), but WAXS crystalline reflections were only observed for EDCP3.5 and ENB19.3. The value of the 2θ halo peak is plotted vs the content of branch points per 100 carbons in the main chain in Figure 12 for quenched and annealed samples. For comparative purposes the data for the series of ethylene−1-decenes is also plotted in this figure. We first notice that, in agreement with the results obtained for the ethylene−1-decenes, the

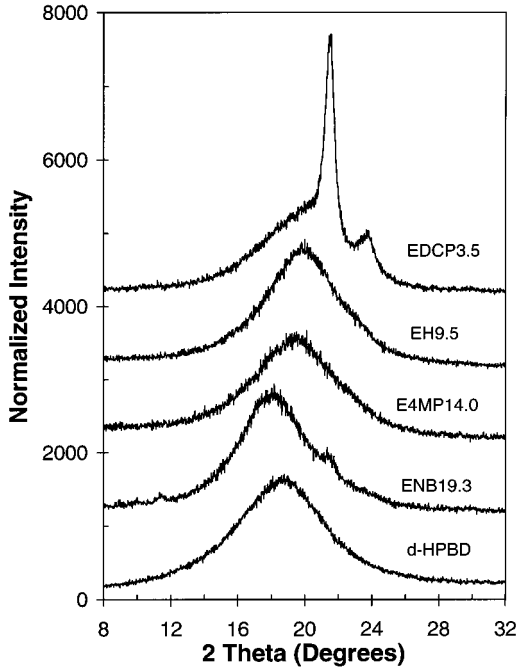

Figure 11. WAXS profiles of ethylene−dicyclopentadiene, ethylene−l-hexene, ethylene−4-methyl-l-pentene, ethylene−norbornene, and deuterated hydrogenated polybutadiene. All copolymers were rapidly crystallized from the melt to 23 °C. WAXS profiles were normalized to the same total area.

annealed copolymers show very similar 2θ halo values and similar degrees of crystallinity by WAXS to the values obtained for the quenched samples.

The 2θ halo of three of these copolymers deviate significantly from the relation obtained for ethylene−1-decenes. Deviations of *d*-HDBD are attributed to the presence of the deuterium atoms. A relatively low value of 2θ halo for ENB19.3 is explained on the basis of the compositional characteristics of this copolymer. The melting thermograms of quenched ENB19.3 and *d*-HPBD (closest in composition) are shown in Figure 13. The double melting of ENB19.3 clearly indicates that this sample has a bimodal branching composition and shows two endotherms at ∼105 and ∼30 °C. The melting temperature of 105 °C is a rather high value for a random copolymer with an overall branching composition of 9.65 mol % branches[38] and is indicative of the presence of a fractional content of molecules with a much lower branching content. Both endotherms become better developed upon annealing. In comparison, the model *d*-HPBD does not show any endothermic transition as corresponding to the behavior of a copolymer with an average composition representative of the single-chain composition. The *d*-HPBD was obtained by anionic polymerization[55] which leads to ethylene−1-butene copolymers with uniform intermolecular branching composition. The insertion of the norbornene group was obviously not homogeneous and led to two populations of chains each with very different average branching content. Melting at the relatively high temperature of 105 °C is attributed to the population of very lightly branched chains that can crystallize even when the overall branch content is high. Since the amorphous region includes all the branches, the overall effective branching for intermolecular distance is higher than the average value of the copolymer with a homogeneous composition. This explains the relatively low value of 2θ halo of this copolymer. On the other hand, one may

Table 3. WAXS Data of Quenched and Annealed Ethylene Copolymers

sample	mol % comonomer	sample	$2\theta_{110}$	$2\theta_{200}$	X_c(WAXS)[b] (%)	2θ halo	$(1-\lambda)_{\Delta H}$[c] (%)
EDCP3.5	3.5	quenched in tap water	21.49	23.74	28.9	19.72	25.3
		annealed at 23 °C	21.43	23.68	29.1	19.69	28.7
EH9.5	9.5	quenched in tap water				19.90	8.9
		annealed at 23 °C				19.90	12.7
E4-MP14.0	14.0	quenched in tap water				19.42	9.0
		annealed at 23 °C				19.49	NA
ENB19.3	19.3	quenched in tap water	21.38	23.58	6.8	18.00	1.4
		annealed at 23 °C	21.26	23.42	8.5	17.77	5.0
d-HPBD	10.6[a]	quenched in tap water				18.56	0
		annealed at 23 °C				18.52	~2.0

[a] Concentration of ethyl branches. [b] Crystallinity calculated from WAXS diffractograms. [c] Crystallinity calculated from heat of fusion measurements.

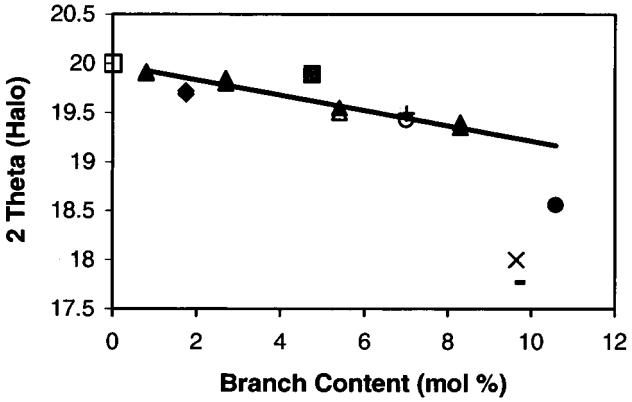

Figure 12. Value of 2θ halo as a function of branching content for ethylene copolymers with different type of comonomer (closed symbols, quenched; open symbols, annealed): ▲, △, 1-decene; ○, +, 4-methylpentene (circle quenched, cross annealed); ◆, ◇, ethylene−dicyclopentadiene; ■, □, ethylene−1-hexene; ●, *d*-HPBD; ×, −, ethylene−norbornene (cross, quenched; line, annealed), □, linear polyethylene. The solid line represents the variation of the 1-decene series and is taken from Figure 7A.

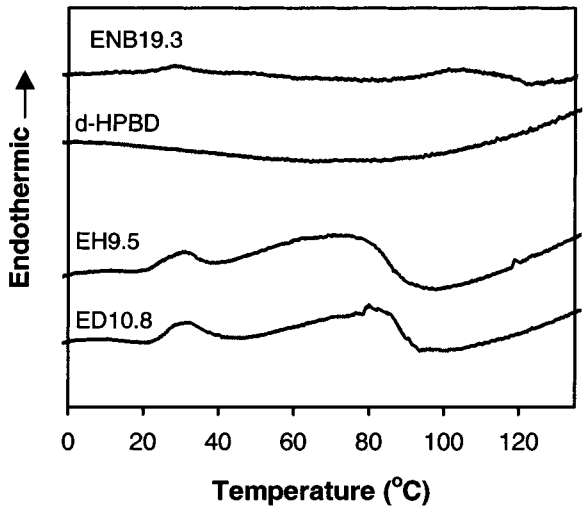

Figure 13. Comparison of DSC thermograms of rapidly crystallized EN19.3 and *d*-HPBD (9.65 and 10.6 mol % branches, respectively) and EH9.5 and ED10.8 (4.75 and 5.4 mol % branches, respectively).

expect that bulkier branches less flexible than the octyl branch of the 1-decene copolymers would lead to a larger average backbone intermolecular distance than that of the 1-alkene branch type and, thus, to a lower 2θ halo. This effect is reflected in the 19.7° value of EDCP3.5 which falls below the average value of the ethylene−1-decene series (see Figure 12).

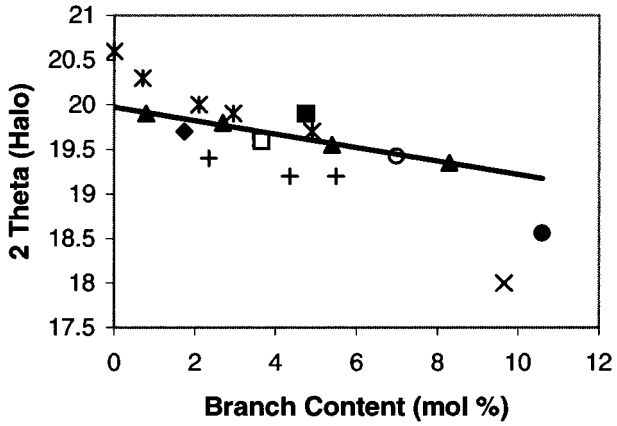

Figure 14. This work and published data of 2θ halo for different ethylene copolymers. This work (quenched samples): ethylene−1-decenes (▲), ethylene−4-methyl-1-pentene (○), ethylene−dicyclopentadiene (◆), ethylene−1-hexene (■), ethylene−norbornene (×), *d*-HPBD (●); literature data: Russell et al.[13,56] (∗), Perez et al.[48] (+), Androsch et al.[16] (□). The solid line represents the variation of the 1-decene series and is taken from Figure 7A.

The EH9.5 copolymer has an anomalous behavior for which we could not give an explanation based on composition or structural details. Compared to ethylene 1-decene with a closely matched composition (see two lower endotherms of Figure 13), the melting curves are basically identical and correspond to the expected behavior for compositionally homogeneous copolymers. A feature that we could not explain is the fact that neither the quenched nor annealed copolymer showed crystalline diffractions. This copolymer was unusually sticky, and any attempts to extract any possible residual monomer or very low molecular weight residues by solvent extraction were not successful.

A compilation of literature data for the peak 2θ halo of different ethylene copolymers and those of the quench samples studied here is given in Figure 14. The line is reproduced from Figure 7a and represents the decrease in 2θ halo with comonomer concentration obtained for ethylene−1-decenes. A similar trend is observed in the data extracted from the works of Russell et al.,[13,56] who studied ethylene−1-butenes, ethylene−1-octenes, and ethylene−1-octadecenes and from the work of Perez et al. for ethylene−1-octadecenes.[48] The numerical differences with the data obtained in this work, higher (Russell) and lower (Perez), are attributed to differences in the calibration method or in the crystallization mode. The 2θ halo of a slowly cooled ethylene−1-octene reported by Androsch et al.[16] follows the behavior of the ethylene−1-decenes. Reported data and that of this

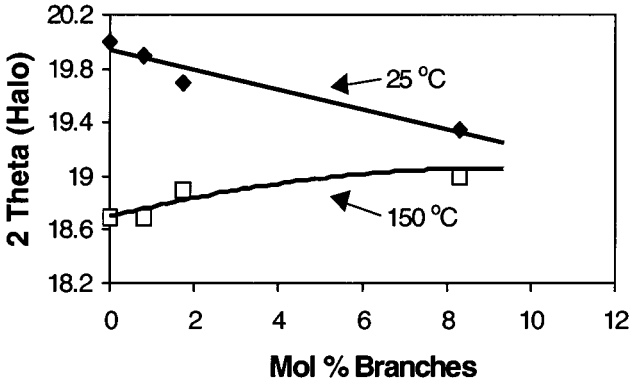

Figure 15. Variation of 2θ halo peak for different copolymers measured at 23 and 150 °C as a function of the copolymer branching content.

work systematically indicate that the angular position of the amorphous halo of rapidly crystallized ethylene copolymers scales in inverse proportion with comonomer content. The continuity in the peak of 2θ halo from crystalline to amorphous copolymers reflects changes associated with the amorphous phase.

Figure 15 compares the 2θ amorphous peak for semicrystalline and amorphous copolymers measured at 23 and at 150 °C. Except for the deuterated copolymer and the bimodal ethylene norbornene, the values obtained at 150 °C follow the density variation of hydrogenated polybutadienes[53] and increase from 18.7° for the linear polymer to 19° for ED16.6. In this comonomer concentration range the variation of the 2θ halo is inverse to that shown at 23 °C. The difference is attributed to the fact that both concentration of comonomer and temperature have an effect on the 2θ value. Figure 15 suggests that the temperature coefficient of the 2θ halo is a function of the comonomer concentration with the least branched copolymers having the highest variation. As a result of both contributions, the temperature variation of the 2θ halo of semicrystalline copolymers is predicted to be nonlinear, especially in the range of temperatures in which both crystalline and amorphous phases coexist. In fact, reported data on ethylene−1-octenes[14] and ethylene−1-butene copolymers[13] support this prediction. The nonlinearity and the steeper slope at low temperatures (see Figure 5A of ref 14 and Figure 3 of ref 13) are now explained by the effect on 2θ of the changing branching composition in the melt with a progressive increase of temperature. When all crystallites are molten, the comonomer composition is constant, and the value of 2θ is only affected by the temperature change.

On the Formation of a Pseudohexagonal Phase. A recent work by Androsch et al.[16] reported, in addition to the 110 and 200 reflections of the orthorhombic phase, an additional reflection at 19.6° for a slowlly cooled ethylene−1-octene copolymer with 7.3 mol % comonomer. This additional reflection is superimposed onto the amorphous halo, and as seen in Figure 14, the peak fits the 2θ−composition relation obtained for ethylene−1-decenes in this work. On the basis of the work of Ballasteros et al.,[26] who unambiguously identified the formation of a hexagonal phase (as the 100 reflection at 4.43 Å) in an ethylene−propylene copolymer, Androsch et al. speculated that the 19.6° reflection was due to the formation of a pseudohexagonal phase with side hexyl branches participating in the crystal-

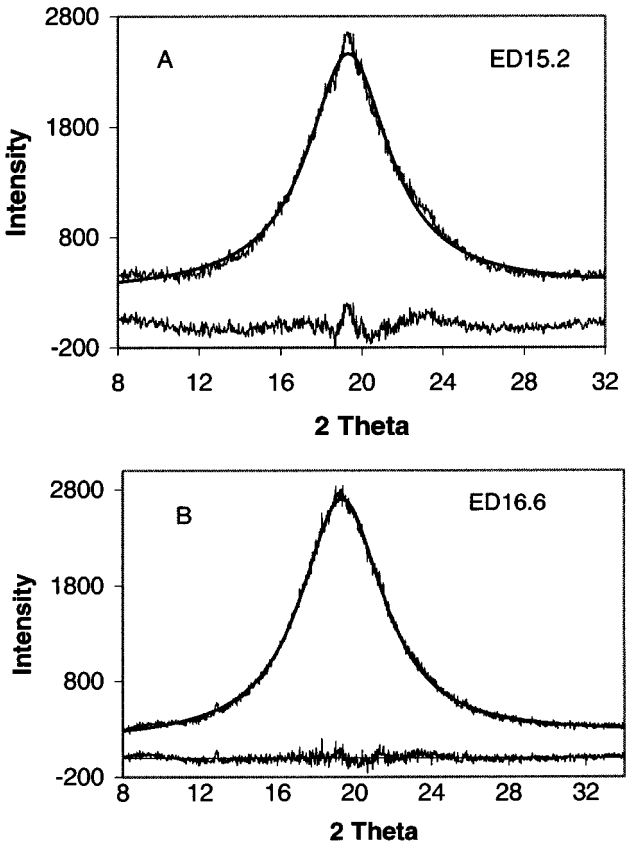

Figure 16. (A) Experimental and fitted WAXS profiles of ethylene−1-decene (15.2 mol % 1-decene) quenched and annealed at 23 °C for 6 months. (B) WAXS profile of ethylene−1-decene (16.6 mol % 1-decene) quenched and annealed at 23 °C for 1 month. The difference between the experimental and calculated profiles is also plotted.

lization process. In an earlier work Russell et al.[13,56] also reported an extra diffraction superimposed in the halo of ethylene−1-octene (15 mol % comonomer) and ethylene−1-octadecene copolymers (5−10 mol % comonomer). However, the extra diffraction was not found in the series of ethylene−1-octadecene copolymers studied by Perez et al.[48] In view of the discrepancies about this additional phase, we sought the reasons for which the copolymers that we studied did not show any indication of the superimposed reflection in the halo even for comonomer concentrations in the range studied by Androsch et al. (see Figure 1). Two weeks annealing at 23 °C or slow crystallizations, which may enhance crystallization of short methylene sequences, did not increase the relative intensity of the halo compared to the quenched copolymers. However, an ethylene−1-decene with 15.2 mol % decene that was quenched and annealed at 23 °C for 6 months shows the diffractogram of Figure 16a. For comparison, the diffractogram of quenched and 1 month annealed ED16.6 is given in Figure 16b. This diffractogram is identical to that shown in Figure 1 for the quenched sample. Crystalline reflections were absent in the sample annealed for an extended period of time, but it was not possible to fit the amorphous halo to a single mixed profile as it was with the copolymers quenched or annealed for up to 1 month. In conclusion, only after very long annealing times the random copolymers developed a poorly ordered crystalline structure consistent with the reported pseudohexagonal phase with rotational symmetry. The formation of these poorly

formed crystallites must be the consequence of slow kinetics in the crystallization of short ethylene sequences from the backbone and possibly from the branch as already reported.[13,16] Logically, the formation of this structure will be favored in ethylene−propylene copolymers[26] in which the methyl branches are partially accommodated in the crystal along with continuous methylenic sequences.

When the same diffractograms of quenched ethylene−decenes of Figure 1 are plotted in an arbitrary not normalized scale, those with the highest comonomer content appear as if they had a peak superimposed on to the amorphous halo. Normalization by total area removes this artifact in our samples (Figure 1). The linear correlation found in Figure 7 for 2θ halo with comonomer concentration, for amorphous and crystalline copolymers, does not support any significant side branch crystallization in the copolymers analyzed in this work.

Conclusions

The crystalline reflections and amorphous halo of the diffractograms of a large number of random ethylene copolymers were analyzed as a function of comonomer concentration and type. Independent of the type of comonomer, a shift in the (110) and (200) peak position is found with increasing comonomer concentration. The lattice expansion is a consequence of the strain caused to thin crystallites by the accumulation of comonomer on the surface of the crystals. Only crystalline reflections corresponding to the orthorhombic structure were identified in these copolymers. The angular position of the amorphous halo of quenched copolymers was found to decrease proportionally to the average concentration of comonomer in the chain. It also scales linearly with the concentration of comonomer in the intercrystalline amorphous region. This variation reflects the increase in average backbone carbon−carbon intermolecular distance with increasing branching content in this region.

Annealing at 23 °C for up to 1 month leads to some increase in crystallinity, but the effect on the halo is insignificant. The 2θ halo peak of isothermally crystallized samples shifts to lower values compared to those of quenched copolymers and reflects a greater change in the melt composition. The effect of changing comonomer concentration on the angular position of the halo is added to the thermal expansion as the temperature of the semicrystalline copolymer is raised. The progressive melting of crystallites with increasing temperature changes the comonomer composition of the amorphous region and leads to a temperature coefficient of the peak position of the halo that is a function of the concentration of comonomer in the chain.

Acknowledgment. The authors acknowledge Dr. D. J. Lohse of the Corporate and Strategic Research of Exxon-Mobil for stimulating and valuable discussions and for providing the *d*-HPBD sample. Support of this work by the National Science Foundation, Polymer Program (DMR-0094485), is gratefully acknowledged. A. G. Simanke acknowledges a scholarship provided by CAPES (Brazil). We also thank Dr. Eric Lochner of the Materials Research and Technology Center of the Florida State University (MARTECH) for helping with the acquisition of WAXS data.

References and Notes

(1) Alexander, L. E. *X-ray Diffraction Methods in Polymer Science*; Wiley-Interscience: New York, 1969; p 137.
(2) Ver Strate, G.; Wilchinsky, Z. W. *J. Polym. Sci.* **1971**, *Part A-2*, 127.
(3) Murthy, N. S.; Minor, H. *Polymer* **1990**, *31*, 996.
(4) Balta-Calleja, F. J.; Vonk, C. G. *X-Ray Scattering of Synthetic Polymers*; Polymer Science Library; Elsevier: Amsterdam, 1989.
(5) Heink, M.; Häberle, K.-D.; Wilke, W. *Colloid Polym. Sci.* **1991**, *269*, 675.
(6) Ruland, W. *Acta Crystallogr.* **1961**, *14*, 1180.
(7) Vonk, C. G. *J. Appl. Crystallogr.* **1973**, *6*, 148.
(8) Turner-Jones, A. *Makromol. Chem.* **1964**, *71*, 1.
(9) Kim, M. H.; Londono, J. D.; Habenschuss, A. *J. Polym. Sci., Polym. Phys. Ed.* **2000**, *38*, 2480.
(10) Voigt-Martin, I.; Wendorff, J. H. In *Encyclopedia of Polymer Science and Engineering*, 2nd ed.; Mark, H. F., Bikales, N. M., Overberger, C. G., Menges, G., Eds.; Wiley: New York, 1985; Vol. 1, p 789.
(11) Rabiej, S. *Eur. Polym. J.* **1991**, *27*, 947.
(12) Russell, K. E.; Hunter, B. K.; Heyding, R. D. *Eur. Polym. J.* **1993**, *2/3*, 211.
(13) McFaddin, D. C.; Russell, K. E.; Wu, G.; Heyding, R. D. *J. Polym. Sci., Polym. Phys. Ed.* **1993**, *31*, 175.
(14) Monar, K.; Habenschus, A. *J. Polym. Sci., Polym. Phys. Ed.* **1999**, *37*, 3401.
(15) Baker, A. M. E.; Windle A. H. *Polymer* **2001**, *42*, 667.
(16) Androsch, R.; Blackwell, J.; Chvalun, S. N.; Wunderlich, B. *Macromolecules* **1999**, *32*, 3740.
(17) Alizadeh, A.; Richardson, L.; Xu, J.; McCarney, S.; Marand, H.; Cheung, Y. W.; Chum, S. P. *Macromolecules* **1999**, *32*, 6221.
(18) Yoon, D. Y.; Flory, P. J. *Faraday Discuss. Chem. Soc.* **1979**, *68*, 288.
(19) Mandelkern, L. *CHEMTRACS−Macromol. Chem.* **1992**, *3*, 347.
(20) Ovchinnikov, Y. K.; Kuz'min, N. N.; Markova, G. S.; Bakeyev, N. F. *Polym. Sci. USSR* **1979**, *20*, 1959.
(21) Bartczak, Z.; Galeski, A.; Argon, A. S.; Cohen, R. E. *Polymer* **1996**, *37*, 2123.
(22) Ovchinnikov, Y. K.; Markova, G. S.; Kargin, V. A. *Polym. Sci. USSR* **1969**, *11*, 369.
(23) Gurato, G.; Fichera, A.; Grandi, F. Z.; Zanetti, R.; Canal, P. *Makromol. Chem.* **1974**, *175*, 953.
(24) Kan, S.; Seto, T. *Rep. Prog. Polym. Phys. Jpn.* **1976**, *19*, 219.
(25) Androsch, R. *Polymer* **1999**, *40*, 2805.
(26) De Ballesteros, O. R.; Auriemma, F.; Guerra, G.; Corradini, P. *Macromolecules* **1996**, *29*, 7141.
(27) Failla, M.; Alamo, R. G.; Mandelkern, L. *Polym. Testing* **1992**, *11*, 151.
(28) Snyder, R. G.; Schlotter, N. E.; Alamo, R.; Mandelkern, L. *Macromolecules* **1986**, *19*, 621.
(29) Mandelkern, L.; Alamo, R.; Mattice, W. L.; Snyder, R. G. *Macromolecules* **1986**, *19*, 2404.
(30) Carella, J. M.; Graessley, W. W.; Fetters, L. J. *Macromolecules* **1984**, *17*, 2775.
(31) Mattice, W. L. *Macromolecules* **1986**, *19*, 2303.
(32) Quijada, R.; Dupont, J.; Miranda, M. L.; Scipioni, R.; Galland, G. B. *Macromol. Chem. Phys.* **1995**, *196*, 3991.
(33) Quijada, R.; Galland, G. B.; Mauler, R. S. *Macromol. Chem. Phys.* **1996**, *197*, 3091.
(34) Alamo, R. G.; Krishnamoorti, R.; Lohse, D. J.; Londono, J. D.; Mandelkern, L.; Stehling, F. C.; Wignall, G. D. *Macromolecules* **1997**, *30*, 561.
(35) Balta-Calleja, F. J.; Vonk, C. G. *X-Ray Scattering of Synthetic Polymers*; Elsevier: New York, 1989.
(36) GRAMS stands for "Graphic Relational Array Management System" by Galactic Industries Corporation, Salem, NH, 1996.
(37) Quinn, F. A., Jr.; Mandelkern, L. *J. Am. Chem. Soc.* **1958**, *80*, 3178.
(38) Alamo, R.; Domszy, R. C.; Mandelkern, L. *J. Phys. Chem.* **1984**, *88*, 6587.
(39) Bunn, C. W., Renfew, A., Morgan, P., Eds. *Polyethylene*; Illife: London, 1975; Chapter 5.
(40) Davis, G. T.; Weeks, J. J.; Martin, G. M.; Eby, R. K. *J. Appl. Phys.* **1974**, *45*, 4175.
(41) Vonk, C. G. In *Integration of Fundamental Polymer Science and Technology*; Lemstra, P. J., Kleintjens, L. A., Eds.; Elsevier: London, 1988; Vol. 2, p 363.
(42) Alamo, R. G.; Mandelkern, L. *Thermochim. Acta* **1994**, *238*, 155.

(43) Chi^2 is a measure of the goodness of fit. It is defined as $\chi^2 = \{\sum_{i=0}^{n}[(\text{actual}_i - \text{calculated}_i)/\text{rms noise}]^2\}/(n - f)$. In this expression i is the number of peaks and $n - f$ the number of degrees of freedom. The actual and calculated values are the measured and calculated areas.
(44) Eichhorn, R. M. *J. Polym. Sci.* **1958**, *56*, 197.
(45) Swan, P. R. *J. Polym. Sci.* **1962**, *56*, 409.
(46) Cole, E. A.; Holmes, D. R. *J. Polym. Sci.* **1960**, *46*, 245.
(47) Shirayama, K.; Kita, S. I.; Watabe, H. *Makromol. Chem.* **1972**, *151*, 97.
(48) Perez, E.; Benavente, R.; Quijada, R.; Narvaez, A.; Barrera-Galland, G. *J. Polym. Sci., Polym. Phys.* **2000**, *38*, 1440.
(49) Alamo R. G.; Mandelkern, L. *Macromolecules* **1991**, *24*, 6480.
(50) Mandelkern, L. *Polym. J.* **1985**, *17*, 337.
(51) Peeters, M.; Goderis, B.; Vonk, C. Reynaers, H.; Mathot, V. B. F. *J. Polym. Sci., Polym. Phys.* **1997**, *35*, 2689.
(52) Mathot, V. B. F.; Pijpers, M. F. J. *J. Therm. Anal.* **1983**, *28*, 349.
(53) Fetters, L. J.; Lohse, D. J.; Colby, R. H. In *Physical Properties of Polymers Handbook*; Mark, J. E., Ed.; American Institute of Physics: New York, 1996; Chapter 24, p 335.
(54) Simanke, A. G.; Alamo, R. G., to appear.
(55) Rachapudy, H.; Smith, G. G.; Raju, V. R.; Graessley, W. M. *J. Polym. Sci., Polym. Phys. Ed.* **1979**, *17*, 1211.
(56) Russell, K. E.; McFaddin, D. C.; Hunter, B. K.; Heyding, R. D. *J. Polym. Sci., Polym. Phys. Ed.* **1996**, *34*, 2447.

MA0106393